Electronic Supplementary Material (ESI) for ChemComm.
This journal is © The Royal Society of Chemistry 2017

Electronic Supplementary Information for:

Hollow Ag_2S Nanosphere Formation via Electron Beam-Assisted Oxidative Etching of Ag Nanoparticles

Sung Joo Kim[a,b], Kyun Seong Dae[a,b], Jae Yeol Park[a], Jeong Yong Lee[a,b], Jong Min Yuk[a*]*

[a] Materials Science and Engineering, Korea Advanced Institute of Science and Technology, 335 Science Road, Daejeon, 305-701, Republic of Korea

[b] Center for Nanomaterials and Chemical Reactions, Institute of Basic Science (IBS), Daejeon 305-701, Republic of Korea

* Correspondence and requests for materials should be addressed to J.Y.L. (email: j.y.lee@kaist.ac.kr) or J.M.Y. (email: jongmin.yuk@kaist.ac.kr)

EXPERIMENTAL SECTION

GLC Preparation Multi-layer graphene sheets are synthesized by using chemical vapor deposition (CVD) and transferred onto a holey-carbon Au grid, following a previous report[1]. GLC is fabricated by encapsulating Ag NPs (Sigma-Aldrich) and the etching solution, $Mg(TFSI)_2$ (Alfa Aesar) dissolved in diglyme solvent. Approximately 20 μL of ionic liquid solution containing Ag NPs with an average size of 50-150 nm is loaded into the cell. To avoid moisture, the GLC fabrication is conducted in an Ar-filled glovebox where both the moisture and oxygen concentrations are kept below 1 ppm.

In-situ TEM Conventional TEM (JEM-2100F, JEOL and JEM-ARM200F, JEOL) is employed for real-time observation of oxidative etching-induced hollow Ag_2S formation. The accelerating voltage used for in-situ experiment is 200 keV with the electron dose in the range of 138.1 – 992.3 $e^-/Å^2 \cdot s$ depending on the imaging magnification. The entire oxidative etching process is recorded using a screen recording software called OCam. The analysis on time-sequential changes in the projected area of a Ag NP is done using Image-J software. The EDS is employed to perform elemental mapping on a Ag NP both before and after oxidative etching.

Movie S1: The movie shows the Ag_2S hollow nanosphere formation by a stepwise process of 1) sulfide shell growth and 2) the active core hollowing of a Ag nanoparticle. The movie plays at 2x speed.

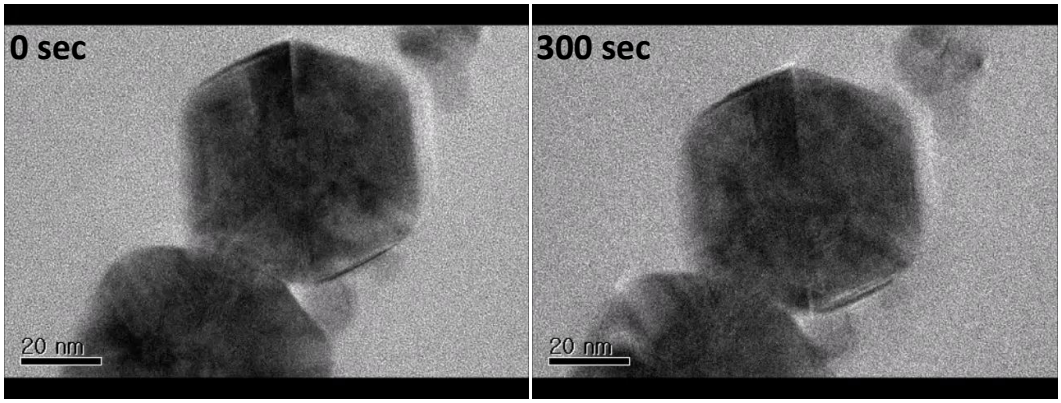

Figure S1. TEM images showing no morphological change of an icosahedral Ag NP in the absence of $TFSI^-$ under electron beam irradiation for 300 seconds.

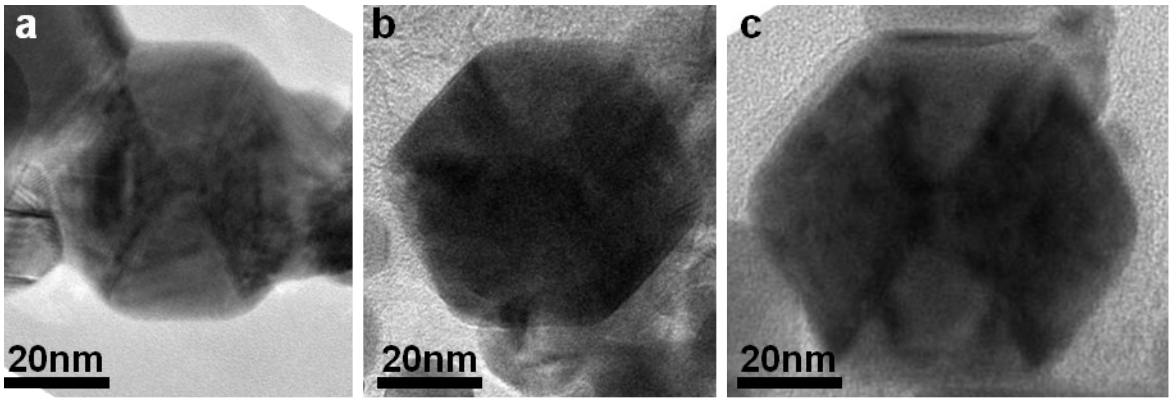

Figure S2. TEM images showing that no morphological change of an icosahedral Ag NP with respect to **(a)** its pristine state is observed **(b)** when the NP is kept inside ionic liquid solution for 2 months and **(c)** when the NP is heated for 8 hours at 90 ^oC.

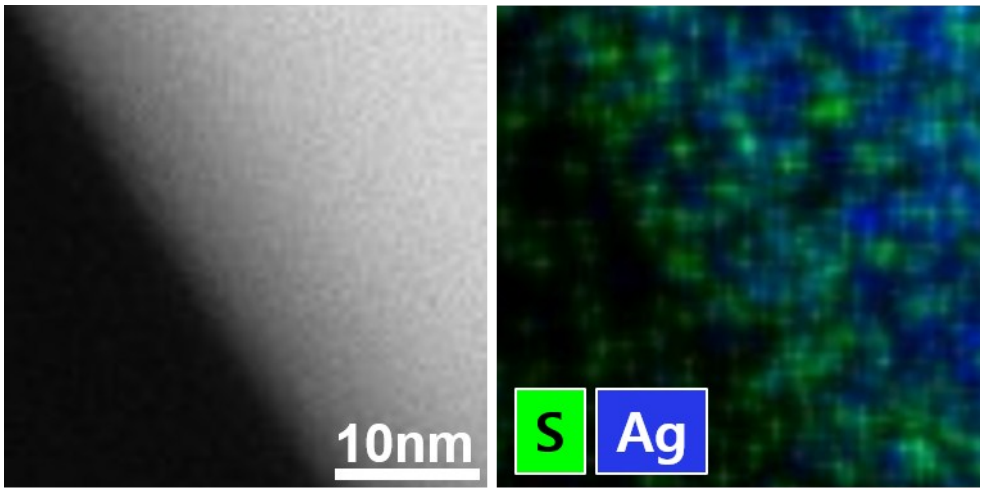

Figure S3. HAADF-STEM image and the corresponding EDS map of a Ag NP inside ionic liquid solution before etching. Note the sulfur species fully surrounding the Ag NP.

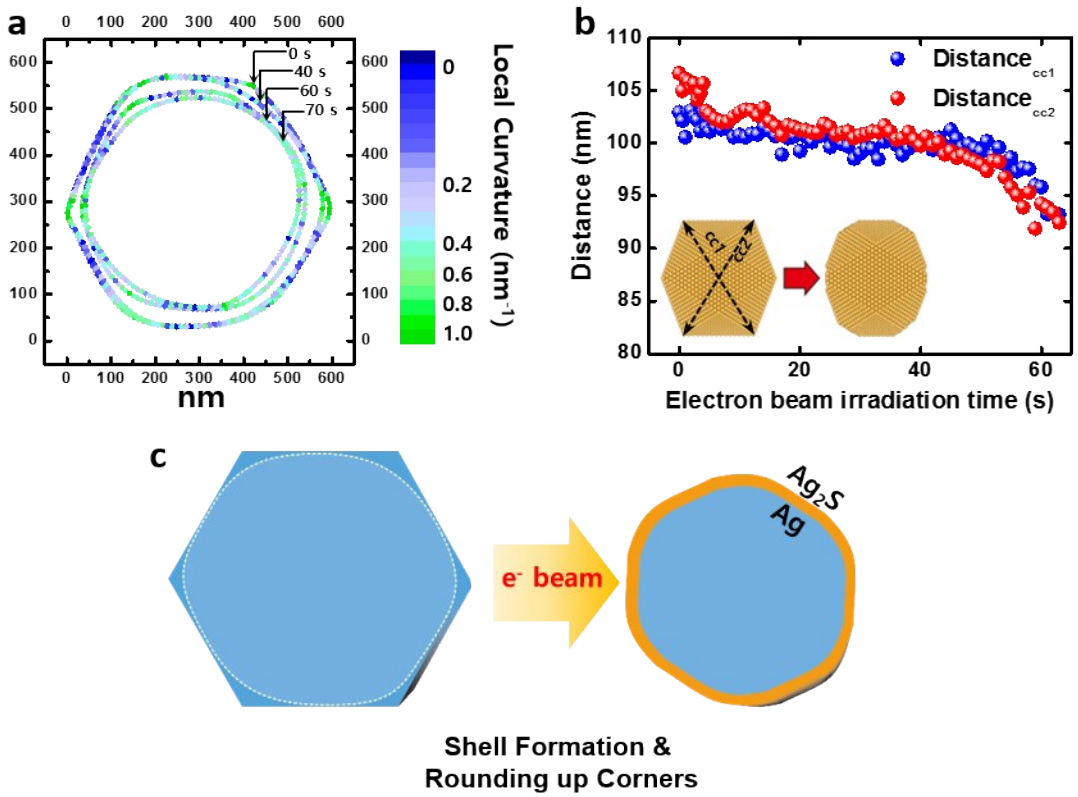

Figure S4. (a) Time-dependent curvature plot of a Ag icosahedron. Note that the original Ag NP already entails the round corners even before the etching since it reaches the certain degree of equilibrium from a kinetic exchange with solution. **(b)** Graph showing changes in corner-to-

corner diameters ($Distance_{cc1}$ & $Distance_{cc2}$) of the Ag NP as a function of electron beam irradiation time. The two selected diameters of the icosahedron are measured for the first 65 seconds at the rate of 1 frame/second. **(c)** Schematic illustration showing Ag_2S shell formation by uniform dissolution of a Ag NP with surface rounding.

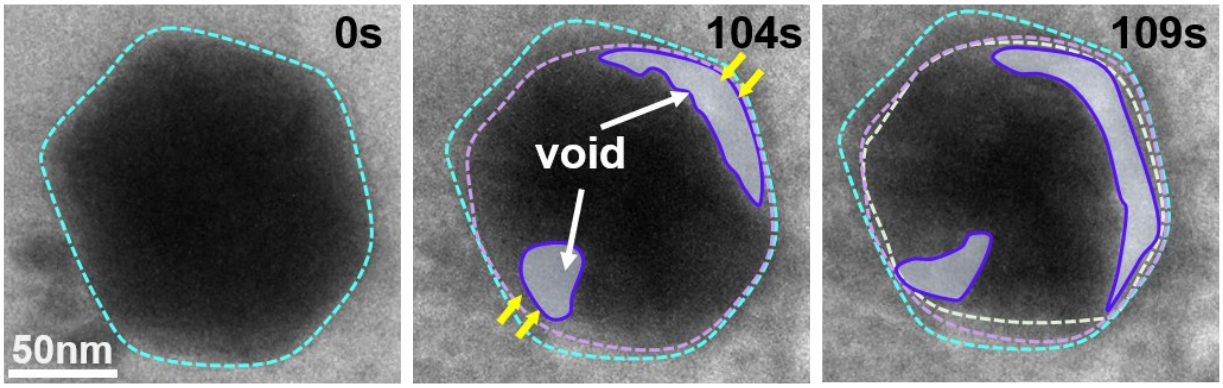

Figure S5. Time-sequential TEM images of an icosahedral NP, which shows that the dissolution starts at two different {110} corners.

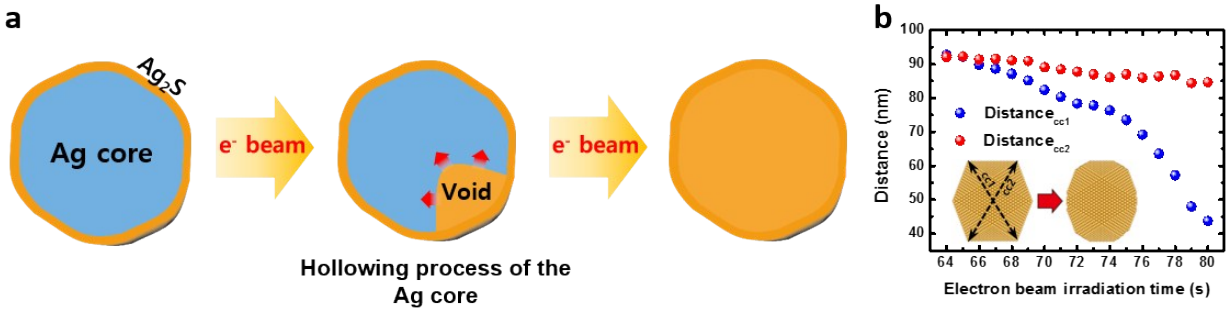

Figure S6. (a, b) Time-sequential TEM images and the corresponding schematic illustration of a Ag NP undergoing the anisotropic inner part hollowing process. **(b)** Graph demonstrating changes in corner-to-corner diameters ($Distance_{cc1}$ & $Distance_{cc2}$) of a Ag-Ag_2S core-shell NP.

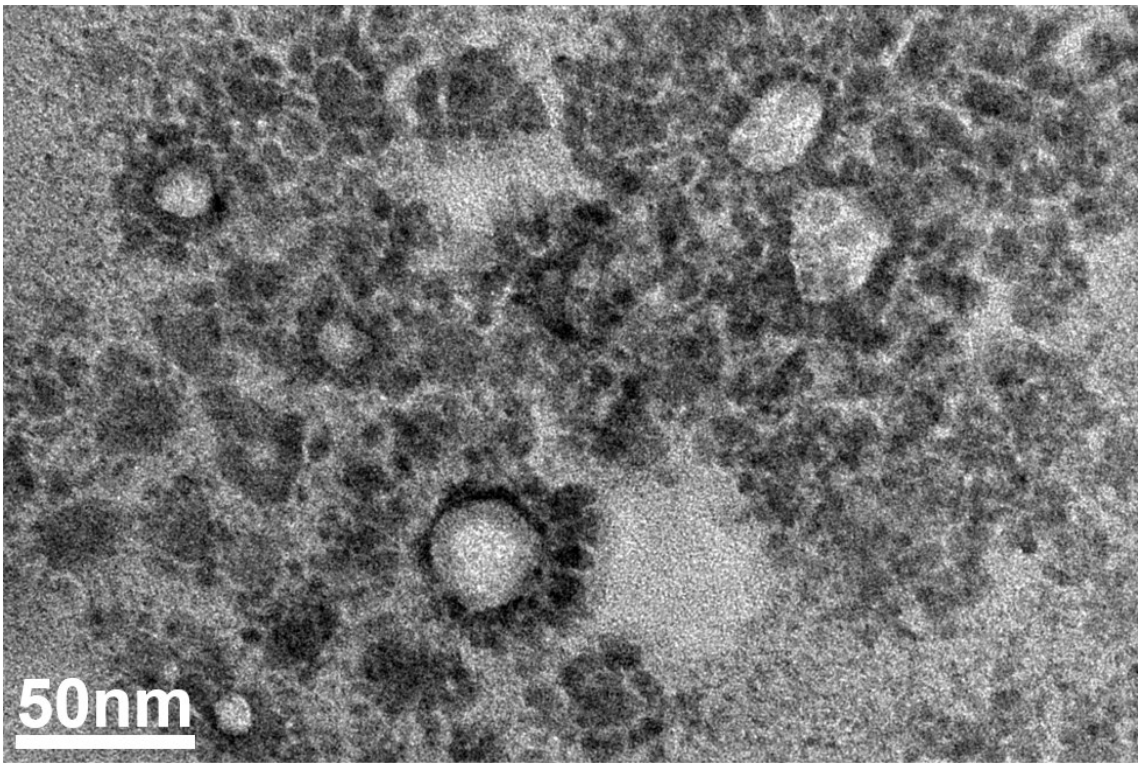

Figure S7. Low-magnification TEM image showing the formation of Ag_2S HNSs from Ag NPs. Note the relative difference in the formation rate of HNSs.

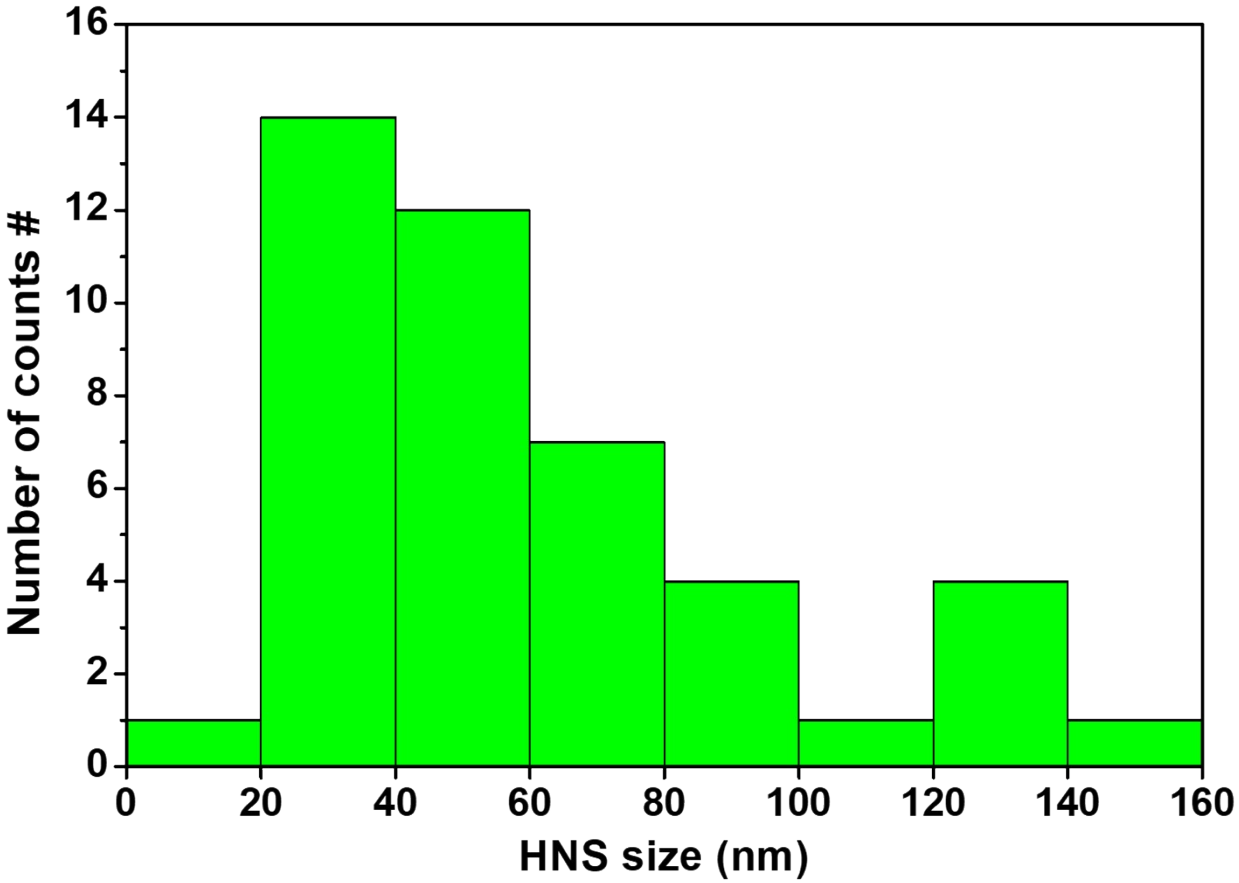

Figure S8. Histogram showing size distribution of Ag_2S HNSs.

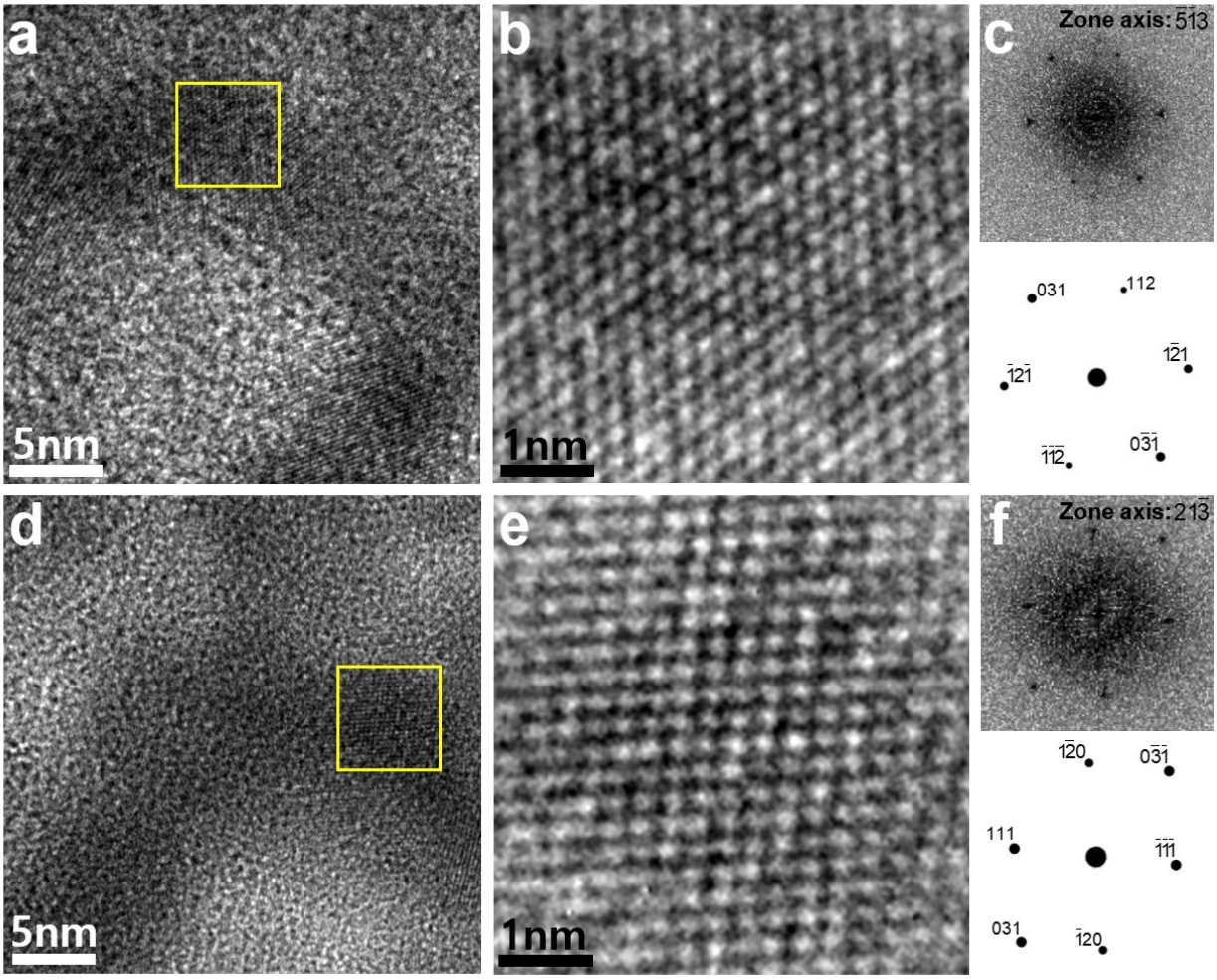

Figure S9. (a and d) HRTEM and (b and e) zoom-in Wiener-filtered images and (c and f) FFT patterns and corresponding simulated patterns of Ag_2S shells from HNSs at different zone axes.

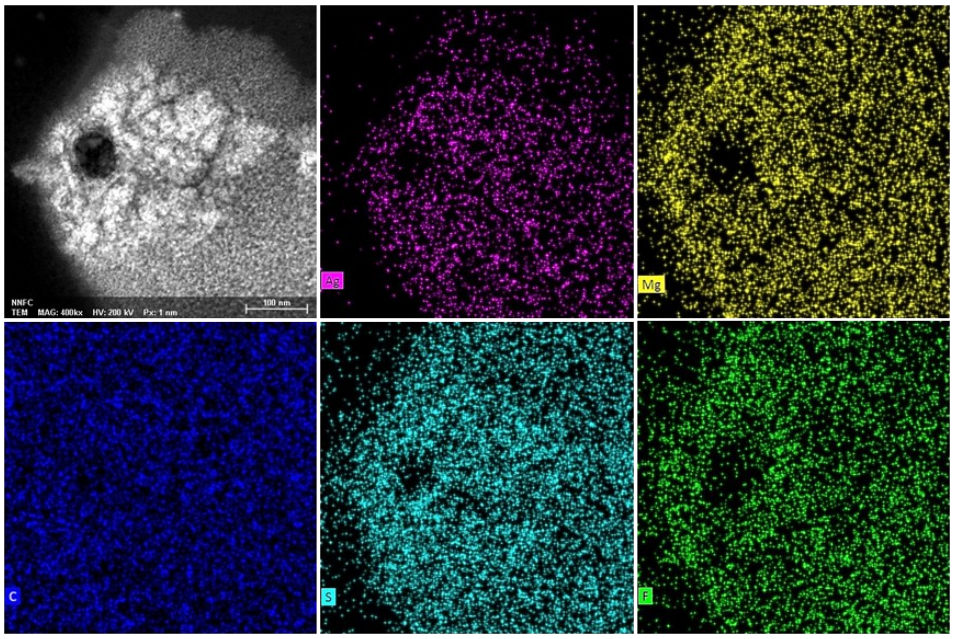

Figure S10. EDS maps of a Ag_2S HNS and its surrounding after electron-beam induced etching.

Appendix A: Finding the dissolution characteristics of Ag NPs

The dissolution characteristics of a Ag NP can be determined from its rate as a function of a radius change. We denote the relationship between the area of a NP after the etching and the reaction time as the following:

$A = A_0 - b\mathrm{t}$, which is the same as:

$r^2 = r_0^2 - b'\mathrm{t}$

$r_0^2 - r^2 = b'\mathrm{t}$

Taking the differential of above with respect to t, we get:

$- 2r \cdot \mathrm{d}r/\mathrm{d}t = b'$

$\mathrm{d}r/\mathrm{d}t = -b'/2r = (-b'/2)\cdot(1/r)$

Hence, dissolution rate $-\mathrm{d}r/\mathrm{d}t$ is proportional to $1/r$, which agrees with the plot in Figure 2c.

Appendix B: Quantiative prediction of a dissolution mechanism

The escaping flux of Ag species from a NP surface towards the solution surrounding NP can simply be defined as:

$$J = \frac{4\pi Dr(r-x)}{x}(c_{int} - c_{esc}) \quad (1)$$

where r is the radius of a NP, x is the diffusion distance of Ag species, c_{int} is the concentration of Ag species at the particle interface with solution, and c_{esc} is the escaping concentration of Ag species from NP. This needs to be comparable to the dissolution flux of Ag species at the NP surface, that is:

$$J = 4\pi r^2 a_d (c_r - c_{int}) \quad (2)$$

where a_{d} is the dissolution rate constant and c_{r} is the Ag concentration inside the NP.

Since $dr/dt = JV_{Ag}/4\pi r^2$, where V_{Ag} is molar volume of Ag, the above expressions can be combined and re-written as:

$$\frac{dr}{dt} = \frac{DV_{Ag}(r-x)(C_r - C_{esc})}{r \cdot x} \Big/ 1 + \frac{D(1-x)}{a_d \cdot r \cdot x}$$

(3)

Now, using the Gibbs-Thompson relationship and assuming $r \ll x$, the equation can further be simplified since concentration is dependent on r, that is:

$$\frac{dr}{dt} = \frac{K \cdot \frac{\frac{1}{r} - \frac{1}{r_{esc}}}{r}}{\frac{1}{D} - \frac{1}{a_d r}} = \frac{K \cdot \frac{1 - \frac{r}{r_{esc}}}{r^2}}{\frac{1}{D} - \frac{1}{a_d r}}$$

(4)

where K is the constant that consists of terms including temperature and the interfacial energy between the particle and the solution. If the dissolution is limited by the interfacial reaction between the NP and the solution ($D \ll a_d r$) and assuming $\frac{r}{r_{esc}}$ is constant, the equation (4) can simply be:

$$\frac{dr}{dt} = -\frac{K \cdot const}{r}$$

Additional References:

(1) Li, X.; Cai, W.; An, J.; Kim, S.; Nah, J.; Yang, D.; Piner, R.; Velamakanni, A.; Jung, I.; Tutuc, E.; Banerjee, S. K.; Colombo, L. ; Ruoff, R. S. Large-Area Synthesis of High-Quality and Uniform Graphene Films on Copper Foils. *Science* **2009**, *324*, 1312-1314